On the observability of activated sludge plants ⋆

Otacílio B. L. Neto * **Michela Mulas** * **Francesco Corona** *,**

* *Postgraduate Programme in Teleinformatics Engineering, Federal University of Ceará, Brazil. (e-mails: minhotmog@alu.ufc.br and {michela.mulas, francesco.corona}@ufc.br)*
** *School of Chemical Engineering, Aalto University, Finland.*

Abstract: In this work, the full-state observability properties of a class of biological wastewater treatment plants are analysed. Specifically, the five biological reactors and the secondary settler in the Benchmark Simulation Model no. 1 are studied. For the task, we represented the activated sludge plant as a dynamical system consisting of 145 states, 8 controls, 14 disturbances and 12 outputs and as a complex network to study its observability properties from a structural and a classical point of view. By analysing the topology of the network, we show how the system is not observable in the structural sense and thus how it is also not observable in the classical sense for all possible realisations of its parameters. As this is also true for a linearisation commonly used in the literature, we analysed a reduced-order system that, based on such linearisation, does not consider the state variables corresponding to dissolved oxygen and alkalinity in the upper-layers of the settler. We show how this system configuration is only observable in a structural sense.

Keywords: Activated sludge process, observability, structural control, complex networks.

1. INTRODUCTION

Wastewater treatment is facing unprecedented challenges due to stricter effluent requirements, costs minimisation, sustainable reuse of water, nutrients and other resources, as well as increasing expectations in the public to attain high service standards. Because of their wide diffusion, activated sludge processes play a key role in the biological treatment of wastewater and their efficient operation and control has a large technological and societal impact.

Many control strategies for activated sludge plants have been proposed in the industrial and academic literature (Olsson et al., 2013). Important research efforts have been possible thank to a number of support tools that provide a simulation protocol for real-world activated sludge processes. The Benchmark Simulation Model no. 1 (BSM1, Gernaey et al. (2014)), specifically, offers a simulation protocol and a general platform for analysing common activated sludge processes subjected to typical municipal wastewater influents. Though the availability of BSMs has stimulated the design of a number of modelling and control solutions, yet too little has been done to study this model and its measurements from a system analytical perspective. To the best of our knowledge, still too few works discuss, for example, state estimation (Busch et al., 2013) and observability (Yin and Liu, 2018) of BSMs.

In this work, the observability properties of a class of activated sludge plants represented by the BSM1 are investigated. For the task, we mapped the dynamical system consisting of 145 state variables, 8 controls, 14 disturbances and 12 outputs onto a complex network in which we studied full-state observability properties of the model from a classical and a structural point of view. As we are primarily interested in determining whether the plant is observable under all feasible linearisations, we studied the structural observability (Lin, 1974; Liu et al., 2013) of the model. The study complements our work on the controllability of this class of models (Neto et al., 2020).

According to our results, BSM1-plants are not structurally observable and thus they are not full-state observable also in a classical sense. As the result is true for almost all linearisations of the nonlinear model, we firstly used structural observability to show that a linearisation commonly used in the literature is not full-state observable, and then we verified the classical counterpart of this result using the Popov-Belevitch-Hautus test (Hautus, 1969). We complete the analysis, by discussing the observability of a reduced-order system with 137 state variables in which dissolved oxygen and alkalinity in the upper layers of the settler are removed. This system is based on the same linearisation and output variables and is only structurally observable.

The work is presented as follows: Section 2 describes an activated sludge plant and its state-space model, Section 3 overviews the classical and structural notion of full-state observability, Section 4 discusses our results on the full-state observability for this class of activated sludge plants.

2. THE ACTIVATED SLUDGE PLANT

We consider the activated sludge process in a conventional wastewater treatment plant. The process consists of five biological reactors and a secondary settler (Fig. 1).

The treatment is based on the denitrification-nitrification process in which bacteria reduce nitrogen present in form

⋆ This work has been done within the international project Control4Reuse, part of the IC4WATER programme, in the frame of the collaborative international consortium of the Water Challenges call 2017, Changing World Joint Programme Initiative (Water JPI).

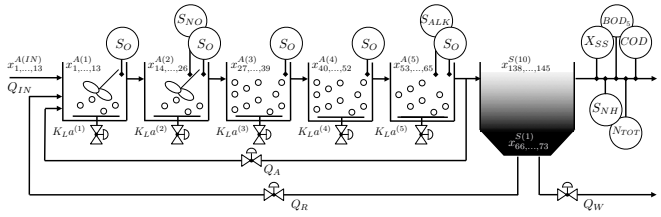

Fig. 1. The activated sludge plant: Process layout.

of nitrate and ammonia in the wastewater into nitrogen gas to be released into the atmosphere. No chemicals are added to the process and only oxygen is potentially added by insufflating air into each reactor. In the aerated reactors, the ammonium nitrogen (NH_4-N) contained in the wastewater is oxidised into nitrate nitrogen (NO_3-N), which is in turn reduced into nitrogen gas in the anoxic reactors. The process begins with a first reactor where wastewater from primary sedimentation, return sludge from secondary sedimentation and internal recycle sludge are fed. The outflow from the first reactor is then sequentially fed to the downstream reactors and, eventually, from the fifth reactor to the secondary settler. Mixed liquor from the fifth reactor is recirculated into the first reactor together with the recycle sludge from secondary sedimentation, as mentioned. Each reactor is described by the Activated Sludge Model no. 1 (Henze et al., 2000), while the settler is represented by the 10-layer non-reactive model proposed by Takács et al. (1991). Under this configuration, the bioprocess corresponds to the Benchmark Simulation Model no. 1 (Gernaey et al., 2014) and it will be referred to as the activated sludge plant.

From the system perspective, the dynamics of each k-th reactor in the activated sludge plant, if studied individually, are represented using 13 state variables, the concentrations

$$x^{A(k)} = \big[S_I^{A(k)}\ S_S^{A(k)}\ X_I^{A(k)}\ X_S^{A(k)}\ X_{BH}^{A(k)}\ X_{BA}^{A(k)}\ X_P^{A(k)}\ S_O^{A(k)}\ S_{NO}^{A(k)}\ S_{NH}^{A(k)}\ S_{ND}^{A(k)}\ X_{ND}^{A(k)}\ S_{ALK}^{A(k)}\big] \quad (k = 1, \ldots, 5),$$

and one controllable input, the oxygen transfer coefficient $u^{(k)} = K_L a^{(k)}$. The dynamics of the m-th layer in the settler are described using 8 state variables, concentrations

$$x^{S(m)} = \big[X_{SS}^{S(m)}\ S_I^{S(m)}\ S_S^{S(m)}\ S_O^{S(m)}\ S_{NO}^{S(m)}\ S_{NH}^{S(m)}\ S_{ND}^{S(m)}\ S_{ALK}^{S(m)}\big] \quad (m = 1, \ldots, 10).$$

Moreover, the activated sludge plant is subjected to three additional controllable inputs, the internal and external sludge recycle flow-rates (Q_A and Q_R, respectively) and the wastage flow-rate Q_W, in addition to 14 uncontrollable inputs or disturbances, the influent flow-rate Q_{IN} and its concentrations $x^{A(IN)}$, all directly implemented in the first reactor. Wastewater concentrations for the internal recycle are given by $x^{A(5)}$, whereas $x^{S(1)}$ are the concentrations within the external recycle and wastage flow. Table 1 provides a brief description of the concentration variables.

As for the measurements, we consider a typical arrangement with a set of sensors measuring the concentrations

$$y = [S_O^{A(1)}\ \cdots\ S_O^{A(5)}\ S_{NO}^{A(2)}\ S_{ALK}^{A(5)}\ X_{SS}^{S(10)}\ S_{NH}^{S(10)}\ BOD_5^{S(10)}\ COD^{S(10)}\ N_{TOT}^{S(10)}].$$

The effluent concentrations of biochemical oxygen demand (BOD_5), chemical oxygen demand (COD) and total nitrogen (N_{TOT}) are defined in terms of state variables to be

$$\begin{aligned} BOD_5^{S(10)} &= ((1 - f_P)(X_{BH}^{S(10)} + X_{BA}^{S(10)}) + S_S^{S(10)} \\ &\quad + X_S^{S(10)})/4; \\ COD^{S(10)} &= S_S^{S(10)} + S_I^{S(10)} + X_S^{S(10)} + X_I^{S(10)} + X_{BH}^{S(10)} \\ &\quad + X_{BA}^{S(10)} + X_P^{S(10)}; \\ N_{TOT}^{S(10)} &= S_{NO}^{S(10)} + S_{NH}^{S(10)} + i_{XB}(X_{BH}^{S(10)} + X_{BA}^{S(10)}) \\ &\quad + S_{ND}^{S(10)} + X_{ND}^{S(10)} + i_{XP}(X_P^{S(10)} + X_I^{S(10)}), \end{aligned}$$

in which the stoichiometric parameters (f_P, i_{XB}, and i_{XP}) are given in Gernaey et al. (2014) and the effluent concentrations $X_a^{S(10)} = (X_{SS}^{S(10)}/X_f)X_a^{A(5)}$ with $a \in \{I, S, BH, BA, P, ND\}$, are computed in terms of $X_f = 0.75(X_I^{A(5)} + X_S^{A(5)} + X_{BH}^{A(5)} + X_{BA}^{A(5)} + X_P^{A(5)})$.

Table 1. Activated sludge plant: Concentrations (state variables and measurements).

	Description (Units)
S_I	Soluble inert organic matter (g COD m^{-3})
S_S	Readily biodegradable substrate (g COD m^{-3})
X_I	Particulate inert organic matter (g COD m^{-3})
X_S	Slowly biodegradable substrate (g COD m^{-3})
X_{BH}	Active heterotrophic biomass (g COD m^{-3})
X_{BA}	Active autotrophic biomass (g COD m^{-3})
X_P	Particulate products from biomass decay (g COD m^{-3})
S_O	Dissolved oxygen (g O_2 m^{-3})
S_{NO}	Nitrate and nitrite nitrogen (g N m^{-3})
S_{NH}	NH_4^+ + NH_3 nitrogen (g N m^{-3})
S_{ND}	Soluble biodegradable organic nitrogen (g N m^{-3})
X_{ND}	Particulate biodegradable organic nitrogen (g N m^{-3})
S_{ALK}	Alkalinity (mol HCO_3^- m^{-3})
X_{SS}	Total suspended solids (g COD m^{-3})
BOD_5	Biochemical oxygen demand (g COD m^{-3})
COD	Chemical oxygen demand (g COD m^{-3})
N_{TOT}	Total nitrogen (g N m^{-3})

The state-space model of the activated sludge plant is

$$\dot{x}(t) = f(x(t), u(t), w(t)|\theta_x) \quad (2a)$$

$$y(t) = g(x(t), u(t), w(t)|\theta_y) \quad (2b)$$

with state variables $x(t) \in \mathbb{R}_{\geq 0}^{N_x} = [x^{A(1)}\ \cdots\ x^{A(5)}\ x^{S(1)}\ \cdots\ x^{S(10)}]^T$, output variables $y(t) \in \mathbb{R}_{\geq 0}^{N_y}$, controllable inputs $u(t) \in \mathbb{R}_{\geq 0}^{N_u} = [Q_A\ Q_R\ Q_W\ K_L a^{(1)}\ \cdots\ K_L a^{(5)}]^T$, uncontrollable inputs $w(t) \in \mathbb{R}_{\geq 0}^{N_w} = [Q_{IN}\ x^{A(IN)}]^T$. The time-invariant dynamics $f(\cdot|\theta_x)$ and $g(\cdot|\theta_y)$ depend on a set of stoichiometric and kinetic parameters θ_x and θ_y (Gernaey et al., 2014). Summarising, we have $N_x = 13 \times 5 + 8 \times 10 = 145$, $N_u = 3 + 5 = 8$ controllable inputs, $N_w = 1 + 13 = 14$ disturbances and $N_y = 12$ outputs.

The default control strategy proposed for the BSM1 consists of two low-level controllers: *i*) nitrate and nitrite nitrogen concentration in the second reactor, $S_{NO}^{A(2)}$, by manipulation of the internal recycle Q_A; *ii*) dissolved oxygen concentration in the fifth reactor, $S_O^{A(5)}$, by manipulation of the oxygen mass transfer coefficient $K_L a^{(5)}$. On a higher level, the performance of the plant is assessed in terms of flow-weighted time-averaged effluent concentrations of total suspended solids (X_{SS}), biochemical oxygen demand (BOD_5), chemical oxygen demand (COD), total nitrogen (N_{TOT}) and ammonia (S_{NH}). Typically, control perfor-

mance is assessed in terms of effluent quality by measuring and minimising the compound effluent concentrations.

The focus of this work is on the full-state observability properties of this common class of activated sludge plants.

3. PRELIMINARIES

Consider a dynamical system, state-space representations

$$\dot{x}(t) = f_t(x(t), u(t), w(t)|\theta_x) \tag{3a}$$
$$y(t) = g_t(x(t), u(t), w(t)|\theta_y) \tag{3b}$$

describe how the state vector $x(t) \in \mathbb{R}^{N_x}$ evolves in time, given its current value and a set of controllable and uncontrollable but measurable input vectors $u(t) \in \mathbb{R}^{N_u}$ and $w(t) \in \mathbb{R}^{N_w}$ - the state equation Eq. (3a) - and how the state vector is emitted to form the measurement vector $y(t) \in \mathbb{R}^{N_y}$ - the measurement equation Eq. (3b). The nonlinear, time-varying and parametric vector functions $f_t(\cdot|\theta_x)$ and $g_t(\cdot|\theta_y)$ define the dynamics and the measurement process, respectively. θ_x and θ_y are the model's parameters. We limit ourselves to time-invariant systems $f(\cdot)$ and $g(\cdot)$ without feedthrough of the inputs and, with no loss of generality we will assume an initial time $t_0 = 0$.

The way state components interact with each other is encoded by a $N_x \times N_x$ matrix A, whereas a $N_x \times N_u$ matrix B captures which state components are affected by the controls and a $N_x \times N_w$ matrix G can be used to identify which state components are affected by the disturbances. Similarly, a $N_y \times N_x$ matrix C can be used to encode the interaction existing between state and output variables.

The structure of matrix A, B, G and C can be determined using inference diagrams in such a way that element $A_{i,j}$ (respectively, $B_{i,j}$, $G_{i,j}$ and $C_{i,j}$) is non-zero and potentially unknown whenever component x_j (u_j, w_j and again x_j) appears in the vector field $f_i(\cdot)$ and algebraic function $g(\cdot)$; that is, whenever the (i,j)-th element $\partial f_i/\partial x_j$ ($\partial f_i/\partial u_j$, $\partial f_i/\partial w_j$ and $\partial g_i/\partial x_j$) in the Jacobian matrix(es) is not identically null. Evaluating the Jacobians at some specific point (x', u', w') leads to a linearised system in which A, B, G and C are assumed to be known and quantify of the strength of the interactions. A steady-state operating point is often used for the linearisation.

The structural nature of the state-space representation of the system can be written using the usual linear model

$$\dot{x}(t) = Ax(t) + Bu(t) + Gw(t) \tag{4a}$$
$$y(t) = Cx(t) \tag{4b}$$

A dynamical system is said to be observable if it is possible to uniquely determine its initial state from a sequence of measurements over a finite time interval. This notion of observability is, in general, a prerequisite for state estimation and, for known linear time-invariant systems, sufficient and necessary observability conditions have been derived from the classical definition by Kalman (1960):

Definition 1. (Observability). The pair (A, C) is said to be observable in the finite time interval $[0, t_f]$ if and only if any initial state $x(0)$ can be determined by the force-free evolution of the output vector $y(t)$ over the same interval.

When matrix A and C are known only structurally, we have to resort to the alternative notion of structural observability and associated sufficient and necessary conditions. In this section, we briefly overview these approaches.

3.1 Classical observability

Let $W_o(t) = \int_0^t e^{A^T\tau} C^T C e^{A\tau} \mathrm{d}\tau$ be the $N_x \times N_x$ observability Gramian of a system (A, C), a sufficient and necessary condition for observability is that $\mathtt{det}(W_o(t)) \neq 0$ for any $t > 0$. Though this criterion allows for a direct determination of the initial state $x(0)$ from the $y(t)$ of minimum quadratic effort or measurement-energy $E(t) \equiv \int_0^t \|y(t)\|^2 \mathrm{d}t$, its computation is unpractical. Equivalently, let $\mathcal{O} = \begin{bmatrix} C^T & A^T C^T & (A^T)^2 C^T & \cdots & (A^T)^{N_x - 1} C^T \end{bmatrix}^T$ be the $\mathbb{R}^{N_y N_x \times N_x}$ observability matrix, a sufficient and necessary condition for observability is that $\mathtt{rank}(\mathcal{O}) = N_x$, $\mathcal{O}$ must be full-rank (Kalman, 1960). This criterion is straightforward and, for low-dimensional systems, its evaluation only requires a small number of matrix multiplications. For high-dimensional state vectors, determining matrix $\mathcal{O}$ is troublesome, as the computation is numerically ill-posed.

A scalable alternative is given by the Popov-Belevitch-Hautus (PBH) observability test, from the Hautus lemma:

Lemma 1. (Hautus, 1969). Let $\sigma(A) = \{\lambda_i\}_{i=1}^{N_x}$ be the spectrum of A. The statement 'the pair (A, C) is observable' and the two following statements are equivalent:

- $\mathtt{rank}(\begin{bmatrix} \lambda I - A^T & C^T \end{bmatrix}^T) = N_x$, $\forall \lambda \in \mathbb{C}$;
- $\mathtt{rank}(\begin{bmatrix} \lambda_i I - A^T & C^T \end{bmatrix}^T) = N_x$, $\forall \lambda_i \in \sigma(A) \subset \mathbb{C}$.

Thus, the pair (A, C) is observable if and only if, for each eigenvalue λ_i of A (that is, when $\mathtt{rank}(\lambda_i I - A^T) < N_x$), the rows of C have at least one component in the state-space direction associated to the eigenvector of A corresponding to λ_i, $\nu_i \in \mathbb{R}^{N_x}$. Eigenvectors ν_i for which $\mathtt{rank}([\lambda_i I - A^T \; C^T]^T) < N_x$ indicate directions that are unobservable through the measurements from matrix C.

3.2 Structural observability

The measurement process of a linear time-invariant system (A, C) can be studied by mapping the state and output equations onto a digraph $\mathcal{G} = (\mathcal{V}, \mathcal{E})$. The vertex set $\mathcal{V} = \mathcal{V}_A \cup \mathcal{V}_C$ consists of the union of vertex set $\mathcal{V}_A = \{x_1, \ldots, x_{N_x}\}$ of state components and of vertex set $\mathcal{V}_C = \{y_1, \ldots, y_{N_y}\}$ of outputs, while the edge set $\mathcal{E} = \mathcal{E}_A \cup \mathcal{E}_C$ is the union of set $\mathcal{E}_A = \{(x_j, x_i) \mid A_{i,j} \neq 0\}$ of directed edges between state component vertices and set $\mathcal{E}_C = \{(x_j, y_k) \mid C_{k,j} \neq 0\}$ of directed edges between state and output components vertices. If the elements of A and C are either zeros or unknown, then the system is referred to as a structured dynamical system (Reinschke, 1988).

The pair (A, C) is said to be structurally observable if the nonzero elements of A and C can be set in such a way that the system is observable in the classical sense. Formally,

Definition 2. (Structural Observability). The pair (A, C) is said to be structurally observable if and only if there exists an observable pair $(\bar{A}, \bar{C})$ of the same dimension and structure of the pair (A, C) such that $\|\bar{A} - A\| < \varepsilon$ and $\|\bar{C} - C\| < \varepsilon$, for an arbitrary small $\varepsilon > 0$.

Two pairs (A, C) and $(\bar{A}, \bar{C})$ have the same structure if they have the same dimensions and each element $A_{i,j} \neq 0$ (respectively, $C_{i,j} \neq 0$) whenever $\bar{A}_{i,j} \neq 0$ ($\bar{C}_{i,j} \neq 0$).

As controllability and observability are dual concepts (Kalman, 1960), the necessary and sufficient conditions for structural observability can be derived from (Lin, 1974):

Lemma 2. Let $\mathcal{G} = (\mathcal{V}, \mathcal{E})$ be the directed network associated to the pair (A, C). (A, C) is said to be structurally observable if and only if the following conditions hold:

- (Accessibility) For every $x_i \in \mathcal{V}_A$ there exists at least one directed path starting from x_i to any $y_k \in \mathcal{V}_C$.
- (Dilation-free) For every $\mathcal{S} \subseteq \mathcal{V}_A$, $|T(\mathcal{S})| \geq |\mathcal{S}|$, where $T(\mathcal{S}) = \{x_j \in \mathcal{V} \mid x_i \in \mathcal{S} \wedge (x_i, x_j) \in \mathcal{E}\}$ denotes a neighborhood set for $\mathcal{S}$.

The first condition can be verified by identifying the output vertices that are accessible from each possible origin vertex (a state component): Any graph search algorithm can be used for the task (Cormen et al., 2009). The second condition can be verified by forming a maximum matching $\mathcal{M} \subseteq \Gamma$ of an equivalent bipartite graph $\mathcal{K} = (\mathcal{V}_A^+ \cup \mathcal{V}_A^-, \Gamma)$ and then checking that all unmatched state vertices $x_j \in \mathcal{V}_A^+$ are directly connected to distinct output vertices in $\mathcal{G} = (\mathcal{V}, \mathcal{E})$ (Liu et al., 2013). The maximum matching problem consists of identifying a (possibly not unique) subset of edges without common vertices that has maximum cardinality. The bipartite graph $\mathcal{K} = (\mathcal{V}_A^+ \cup \mathcal{V}_A^-, \Gamma)$ is defined by the disjoint and independent vertex sets $\mathcal{V}_A^+ = \{x_1^+, \ldots, x_{N_x}^+\}$ and $\mathcal{V}_A^- = \{x_1^-, \ldots, x_{N_x}^-\}$, and by the undirected edge set $\Gamma = \{(x_i^+, x_j^-) \mid (x_i, x_j) \in \mathcal{E}\}$. Unmatched state vertices linked to distinct output vertices form a $\mathcal{V}_A^+-$perfect matching. A guarantee of the dilation-free condition follows from the Hall's theorem (Hall, 1935).

4. RESULTS AND DISCUSSION

In this section, we analyse the full-state observability properties for the class of activated sludge process plants represented by model (2) defined in Section 2. We present the results about the structural observability of the associated structural system (A, C) and then we discuss the classical results obtained for a common linearisation (A^{SS}, C^{SS}). We conclude with the analysis of a reduced-order system.

4.1 Observability of the complete system

For the activated sludge plant $\dot{x}(t) = f(x(t), u(t), w(t)|\theta_x)$ with measurement process $y(t) = g(x(t), u(t), w(t)|\theta_y)$, with $N_x = 145$, $N_y = 12$, $N_u = 8$ and $N_w = 14$, the structural pair (A, C) is obtained from the Jacobian matrices, in such way that $A \in \mathbb{R}^{145\times145} = \partial f/\partial x$ and $C \in \mathbb{R}^{12\times145} = \partial g/\partial x$. The associated digraph $\mathcal{G} = (\mathcal{V}, \mathcal{E})$, in Fig. 2, is defined by the vertex set $\mathcal{V} = \mathcal{V}_A \cup \mathcal{V}_C = \{x_1, \ldots, x_{145}\} \cup \{y_1, \ldots, y_{12}\}$ and the directed edge set $\mathcal{E} = \mathcal{E}_A \cup \mathcal{E}_C = \{(x_j, x_i) \mid A_{i,j} \neq 0\} \cup \{(x_j, y_k) \mid C_{k,j} \neq 0\}$.

The topology of network $\mathcal{G} = (\mathcal{V}, \mathcal{E})$ indicates that the pair (A, C) is structurally unobservable (Lemma 2). As there are no paths from the state vertices $\{S_O^{S(m)}, S_{ALK}^{S(m)}\}_{m=7}^{10}$ to any of the output vertices, the accessibility condition is not satisfied. Conversely, the dilation-free condition is

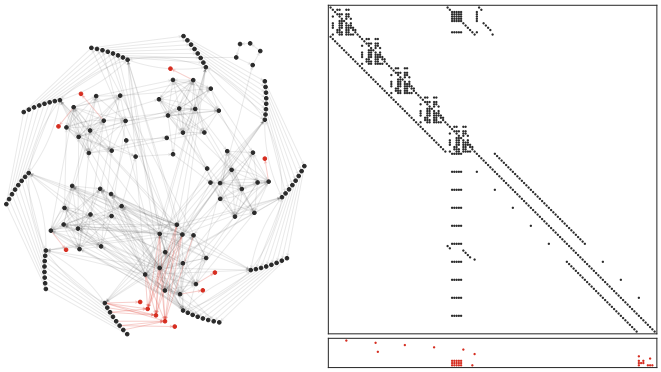

Fig. 2. Network $\mathcal{G} = (\mathcal{V}, \mathcal{E})$, left, and associated structural pair (A, C), right. State vertices $x_i \in \mathcal{V}_A$ are in black, output vertices $y_k \in \mathcal{V}_C$ are in red. State-state edges $(x_i, x_j) \in \mathcal{E}_A$ and state-output edges $(x_i, y_k) \in \mathcal{E}_C$ are dyed to match the corresponding entries in A and C. To reduce clutter, state self-loops have been omitted.

satisfied by the perfect matching $\mathcal{M}$ of size $|\mathcal{M}| = N_x$ obtained by choosing the self-loop associated to each state vertex. The lack of structural observability implies that the system is also not full-state observable in a classical sense. We conclude that for the activated sludge plant given by model (2) it is not possible to determine the initial state $x(0)$, and thus neither intermediate states $x(t)$, starting from a measurement $y(t_f)$. Being of structural nature, the conclusion is valid also in a classical sense, whatever the model linearisation. As a result, it is also not possible to design a full-state-observer based on the existing measurements, no matter what pair (A, C) is used.

For completeness, we consider the linearisation (A^{SS}, C^{SS}) corresponding to the fixed point $(x^{SS}, u^{SS}, w^{SS}, y^{SS})$ considered by Gernaey et al. (2014). This linearisation is commonly utilised in the literature and constitutes the default configuration of the BSM1. We show that this realisation is unobservable also in a classical sense. The pair (A^{SS}, C^{SS}) from the Jacobians evaluated at such equilibrium point (that is, $A^{SS} = \partial f/\partial x|_{SS}$ and $C^{SS} = \partial g/\partial x|_{SS}$) is depicted in Fig. 3, together with the weighted digraph $\mathcal{G}_{SS} = (\mathcal{V}_{SS}, \mathcal{E}_{SS})$ with vertex set $\mathcal{V}_{SS} = \mathcal{V}_{A^{SS}} \cup \mathcal{V}_{C^{SS}} = \{x_1, \ldots, x_{145}\} \cup \{y_1, \ldots, y_{12}\}$ and edge set $\mathcal{E}_{SS} = \mathcal{E}_{A^{SS}} \cup \mathcal{E}_{C^{SS}} = \{(x_j, x_i) \mid A_{i,j}^{SS} \neq 0\} \cup \{(x_j, y_k) \mid C_{k,j}^{SS} \neq 0\}$.

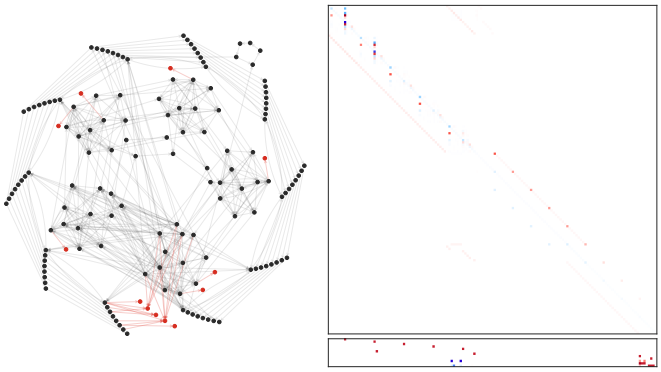

Fig. 3. Network $\mathcal{G}_{SS} = (\mathcal{V}_{SS}, \mathcal{E}_{SS})$, left, associated to pair (A^{SS}, C^{SS}), right. State self-loops have been omitted.

The spectrum $\sigma(A^{SS})$ consists of 69 distinct eigenvalues $\{\lambda_i(A^{SS})\}$, with $\{\lambda_1, \cdots, \lambda_{30}\} \subset \mathbb{R}$ and $\{\lambda_{31}, \lambda_{31}^*, \cdots,$

$\lambda_{69}, \lambda_{69}^*\} \subset \mathbb{C}$. Five complex conjugate pairs of eigenvalues have algebraic multiplicity equal to two and one real eigenvalue has algebraic multiplicity equal to twenty-eight. Being $\texttt{Re}(\lambda_i) < 0$ for all $\lambda_i \in \sigma(A^{SS})$, then A^{SS} is a stable matrix and this plant is considered asymptotically stable.

As expected, also the pair (A^{SS}, B^{SS}) is not full-state observable in a structural sense, as there is no path from the state vertices $\{S_O^{S(m)}, S_{ALK}^{S(m)}\}_{m=7}^{10}$ to any of the output vertices. Again, this result is valid also in the classical sense. The classical counterpart can be verified only by performing the PBH observability test (Lemma 1), as an accurate computation of the observability matrix $\mathcal{O} = [C^{SS^T} A^{SS^T} C^{SS^T} \cdots (A^{SS^T})^{N_x - 1} C^{SS^T}]^T$ is unfeasible.

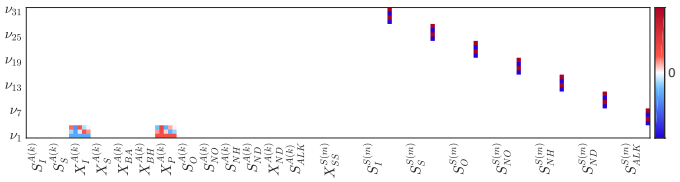

Fig. 4. Pair (A^{SS}, C^{SS}): Eigenvectors $\nu_i(\lambda_i)$ with $\lambda_i \in \sigma(A^{SS})$ such that $\texttt{rank}([\lambda_i I - A^{SS^T}\ C^{SS^T}]^T) < N_x$. Only the real part $\texttt{Re}(\nu_i)$ is being displayed.

The test confirms that the pair (A^{SS}, C^{SS}) is not full-state observable, as 4 distinct eigenvalues, including the real value with multiplicity equal to 28, lead to rank-deficient matrices $[\lambda_i I - A^{SS^T}\ C^{SS^T}]^T$. The 31 eigenvectors associated to such eigenvalues are depicted in Fig. 4. Interestingly, note that the non-zero entries of the 28 eigenvectors associated to the real eigenvalue correspond to state variables relative to soluble matter in the settler's last layer. The other three eigenvectors have non-zero entries only at state variables $\{X_I^{A(k)}\}_{k=1}^5$ and $\{X_P^{A(k)}\}_{k=1}^5$.

4.2 Observability of a reduced-order system

Although not realistic, a structurally observable system can be easily obtained by including, for example, a set of outputs that directly measure the state variables $\{S_O^{S(m)}, S_{ALK}^{S(m)}\}_{m=7}^{10}$; a total of 8 sensors would be required. A more parsimonious solution would be to measure only the state variables corresponding to the leaf nodes of the two directed paths connecting state-vertices $\{S_O^{S(m)}\}_{m=7}^{10}$ and $\{S_{ALK}^{S(m)}\}_{m=7}^{10}$; that is, state variables $S_O^{S(10)}$ and $S_{ALK}^{S(10)}$. Being observable in a structural sense, both such systems would be also full-state observable in a classical sense, for almost all possible linearisations of the model or, equivalently, in the vicinity of all feasible operating points.

Alternatively, it is possible to consider the reduced-order system in which state variables $\{S_O^{S(m)}, S_{ALK}^{S(m)}\}_{m=7}^{10}$ are excluded. As these state variables have decoupled dynamics and, as already pointed out, they are not directly measured, their removal lead to a structurally observable system of smaller size. As full-state observability in the structural sense implies observability in the classical sense for almost all possible realisations of the associated matrix $\widetilde{A} \in \mathbb{R}^{137\times137}$ and $\widetilde{C} \in \mathbb{R}^{12\times137}$, we conclude that such a reduced-order system is therefore almost surely observable.

With this respect, we considered the specific linearisation $(\widetilde{A}^{SS}, \widetilde{C}^{SS})$ of the reduced-order model corresponding to the usual fixed points $(x^{SS}, u^{SS}, w^{SS}, y^{SS})$ considered by (Gernaey et al., 2014). The pair $(\widetilde{A}^{SS}, \widetilde{C}^{SS})$ and its associated digraph $\widetilde{\mathcal{G}}_{SS} = (\widetilde{\mathcal{V}}_{SS}, \widetilde{\mathcal{E}}_{SS})$ are depicted in Fig. 5. In the following we briefly discuss the stability of this realisation and we show that it is unobservable in the classical sense, although observable in the structural sense.

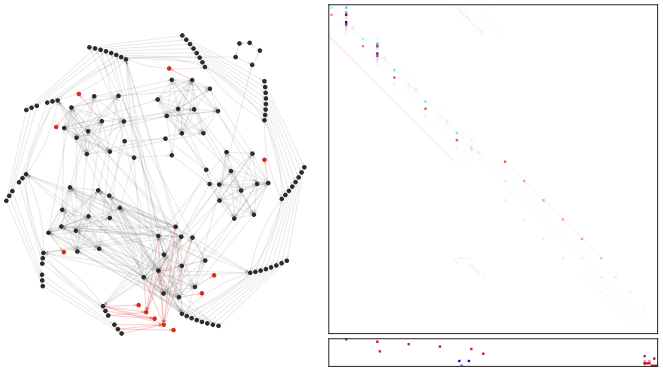

Fig. 5. Network $\widetilde{\mathcal{G}}_{SS} = (\widetilde{\mathcal{V}}_{SS}, \widetilde{\mathcal{E}}_{SS})$, left, associated to pair $(\widetilde{A}^{SS}, \widetilde{C}^{SS})$, right. State self-loops have been omitted.

The spectrum of $\widetilde{A}^{SS}$ consists of 69 distinct eigenvalues $\lambda_i(\widetilde{A}^{SS})$, among which there are five complex conjugate pairs each with algebraic multiplicity equal to two and one real value with algebraic multiplicity equal to twenty. Also in this case, being $\texttt{Re}(\lambda_i(\widetilde{A}^{SS})) < 0$ always negative, this system is considered to be asymptotically stable.

As expected, the pair $(\widetilde{A}^{SS}, \widetilde{C}^{SS})$ is full-state observable in the structural sense (Lemma 2). Conversely, the PBH observability test (Lemma 1) reveals that the same pair is not observable in the classical sense. In fact, being state variables $\{S_O^{S(m)}, S_{ALK}^{S(m)}\}_{m=7}^{10}$ characterised by decoupled dynamics, their exclusion leads to a spectrum $\sigma(\widetilde{A}^{SS})$ that still contains a number of eigenvalues that renders the matrix $[\lambda_i I - \widetilde{A}^{SS^T}\ \widetilde{C}^{SS^T}]^T$ rank-deficient. We can interpret this result by comparison with the pair (A^{SS}, C^{SS}), in which 8 eigenvectors of matrix A^{SS} whose non-zero entries correspond to $S_O^{S(10)}$ and $S_{ALK}^{S(10)}$ and their respective eigenvalues are no longer present, while 20 eigenvectors whose non-zero entries correspond to remaining soluble matter in settler's last layer and 3 eigenvectors whose non-zero entries correspond to $\{X_I^{A(k)}, X_P^{A(k)}\}_{k=1}^5$ are still present.

We conclude that for the activated sludge plant with measurement process given by the pair $(\widetilde{A}^{SS}, \widetilde{C}^{SS})$ it is not possible to determine the initial state $x(0)$, neither intermediate states $x(t)$, starting from measurement $y(t_f)$.

The apparent contradiction between the structural and the classical result can be explained from the analysis of the the dilation-free and accessibility condition applied to the network $\widetilde{\mathcal{G}}_{SS} = (\widetilde{\mathcal{V}}_{SS}, \widetilde{\mathcal{E}}_{SS})$. Specifically, as the existence of a self-loop for each state vertex is sufficient to satisfy this condition, the output vertices are needed only to satisfy the accessibility condition. Whenever some of the self-loop weights are equal, the maximum matching will underestimate the number of output vertices needed for

full-state observability (Zhao et al., 2015). This is the case with $(\widetilde{A}^{SS}, \widetilde{C}^{SS})$, where all settler's soluble components (respectively, all reactors' non-reacting components) from the same layer (unit) always have identical self-dynamics.

The dynamics of the soluble components $\{S_a^{S(7\rightsquigarrow 10)}\}$ with $a \in \{I, S, NO, NH, ND\}$ in the upper layers of the settler are each represented in model (2) by first-order differential equations of the form $\dot{S}_a^{S(m)} = Q_E^{(m)}(S_a^{S(m-1)} - S_a^{S(m)})$ for $m = 7, \ldots, 10$. $Q_E^{(m)}$ denotes the influent flow-rate to the m-th layer. The model assumes the same influent flow-rate for each layer, $\{Q_E^{(m)} = (Q_{IN} - Q_W)/V_S^{(m)}\}_{m=7}^{10}$, and constant volumes $V_S^{(m)} = 600$ m^3. For the relevant entries in the Jacobian matrix $\partial f/\partial x$ of the dynamics, we have

$$\left.\frac{\partial \dot{S}_a^{S(m)}}{\partial S_a^{S(m)}}\right|_{SS} = \left.\frac{Q_W - Q_{IN}}{V_S^{(m)}}\right|_{SS},$$

which is equal for all upper layers ($m = 7, \ldots, 10$), independently of the fixed-point adopted for linearisation.

Similarly, the dynamics of the non-reacting components $\{X_b^{A(1\rightsquigarrow 5)}\}$, with $b \in \{I, P\}$ in the reactors are each represented in (2) by first-order differential equations of the form $\dot{X}_b^{A(k)} = Q^{(k)}(X_b^{A(k-1)} - X_b^{A(k)}) + R_b^{(k)}$ for k=1,...,5. $Q^{(k)}$ denotes the influent flow-rate to the k-th reactor and $R_b^{(k)}$ indicates the contribution from process reactions. The model assumes the same influent flow-rate for each reactor, $\{Q^{(k)} = (Q_A + Q_R + Q_{IN})/V_A^{(k)}\}_{k=1}^{5}$, and constant volumes $V_A^{(1\rightsquigarrow 2)} = 1000$ m^3 and $V_A^{(3\rightsquigarrow 5)} = 1333$ m^3. As $X_b^{A(k)}$ represent non-reacting matter, we have $\partial R_b^{(k)}/\partial X_b^{A(k)} = 0$ and $R_I^{(k)} = 0$. For the relevant entries in the Jacobian $\partial f/\partial x$ of the dynamics, we have

$$\left.\frac{\partial \dot{X}_b^{A(k)}}{\partial X_b^{A(k)}}\right|_{SS} = -\left.\frac{Q_A + Q_R + Q_{IN}}{V_A^{(k)}}\right|_{SS},$$

which is equal for all reactors, whatever the fixed-point.

REFERENCES

Busch, J., Elixmann, D., Kühl, P., Gerkens, C., Schlöder, J.P., Bock, H.G., and Marquardt, W. (2013). State estimation for large-scale wastewater treatment plants. *Water Res.*, 47(13), 4774–4787.

Cormen, T.H., Leiserson, C.E., Rivest, R.L., and Stein, C. (2009). *Introduction to Algorithms*. MIT press.

Gernaey, K., Jeppsson, U., Vanrolleghem, P., and Copp, J. (2014). *Benchmarking of Control Strategies for Wastewater Treatment Plants*. IWA.

Hall, P. (1935). On representatives of subsets. *J. London Math. Soc.*, s1-10(1), 26–30.

Hautus, M. (1969). Controllability and observability conditions of linear autonomous systems. *Indagationes Mathematicae (Proceedings)*, 72(5), 443–448.

Henze, M., Gujer, W., Mino, T., and van Loosdrecht, M.C.M. (2000). *Activated Sludge Models ASM1, ASM2, ASM2d and ASM3*. IWA.

Kalman, R. (1960). On the general theory of control systems. *IFAC Proceedings Volumes*, 1(1), 491 – 502. 1st International IFAC Congress on Automatic and Remote Control, Moscow, USSR, 1960.

Lin, C.T. (1974). Structural controllability. *IEEE Trans. Autom. Control*, 19(3), 201–208.

Liu, Y.Y., Slotine, J.J., and Barabási, A.L. (2013). Observability of complex systems. *Proceedings of the National Academy of Sciences*, 110(7), 2460–2465. doi: 10.1073/pnas.1215508110.

Neto, O., Mulas, M., and Corona, F. (2020). On the controllability of activated sludge plants. In *2020 European Control Conference (ECC)*, to appear.

Olsson, G., Carlsson, B., Comas, J., Copp, J., Gernaey, K., Ingildsen, P., Jeppsson, U., Kim, C., Rieger, L., Rodrìguez-Roda, I., Steyer, J., Takács, I., Vanrolleghem, P., Vargas, A., Yuan, Z., and Åmand, L. (2013). Instrumentation, control and automation in wastewater - from London 1973 to Narbonne 2013. *Water Sci. Technol.*, 69(7), 1372–1385.

Reinschke, K.J. (1988). *Multivariable Control: a Graph-theoretic Approach*. Springer.

Takács, I., Patry, G., and Nolasco, D. (1991). A dynamic model of the clarification-thickening process. *Water Res.*, 25(10), 1263–1271.

Yin, X. and Liu, J. (2018). State estimation of wastewater treatment plants based on model approximation. *Comput. Chem. Eng.*, 111, 79–91.

Zhao, C., Wang, W.X., Liu, Y.Y., and Slotine, J.J. (2015). Intrinsic dynamics induce global symmetry in network controllability. *Sci. Rep.*, 5, 8422.

Appendix A. A SMOOTH APPROXIMATION OF THE SETTLER'S MODEL

To compute Jacobian linearisations, the vector-valued functions f and g must be differentiable. Due to a number of discontinuous functions in the model of the settler, this is not true for the formulation by Gernaey et al. (2014).

A smooth approximation of the original model was obtained by replacing the many terms corresponding to minimum and maximum functions between two terms with a log-sum-exp or softmax function, whereas a logistic function was used for approximating conditional statements.

Specifically, the downward flux of solids in the sixth and higher layers ($m \geq 6$) is defined using conditional functions

$$J_{cla} = \begin{cases} \min(J_s(X_{SS}^{S(m-1)}), J_s(X_{SS}^{S(m)})), & X_{SS}^{S(m-1)} > X_t \\ J_s(X_{SS}^{S(m)}), & \text{elsewhere} \end{cases},$$

with $J_s(X_{SS}^{S(m)}) = v_s(X_{SS}^{S(m)})X_{SS}^{S(m)}$ denoting the gravitational solid flux, settling velocity $v_s(X_{SS}^{S(m)})$, and threshold concentration $X_t = 3000$ g m^{-3}. We rewrite the condition,

$$\begin{aligned} J_{cla} = {} & [1 - \varphi(X_{SS}^{S(m-1)})]J_s(X_{SS}^{S(m)}) \\ & + \varphi(X_{SS}^{S(m-1)}) \min(J_s(X_{SS}^{S(m)}),\ J_s(X_{SS}^{S(m-1)})), \end{aligned}$$

with $\varphi(X_{SS}^{S(m-1)}) = 1$ (respectively, $\varphi(X_{SS}^{S(m-1)}) = 0$) when $X_{SS}^{S(m-1)} - X_t > 0$ ($X_{SS}^{S(m-1)} - X_t \leq 0$). We approximate the step function $\varphi(X_{SS}^{S(m-1)})$ with a logistic function $\varphi(X_{SS}^{S(m-1)}) \approx (1 + e^{-\alpha(X_{SS}^{S(m-1)} - X_t)})^{-1}$, $\alpha = 100$.